Pergamon

Polyhedron Vol. 14, No. 19, pp. 2711–2722, 1995
Elsevier Science Ltd
Printed in Great Britain
0277–5387/95 $9.50+0.00

0277–5387(95)00137–9

THE KINETICS OF TRISBIDENTATE CHELATE COMPLEXES REVISITED. A TWO-DIMENSIONAL NMR STUDY OF THE ISOMERIZATION AND RACEMIZATION PROCESSES OF THE COMPLEXES [M(TTA)$_3$] (M = Al^{III}, Ga^{III}; TTA = 2-THENOYLTRIFLUOROACETONE)*

KENNETH KITE, KEITH G. ORRELL† and VLADIMIR ŠIK

Department of Chemistry, University of Exeter, Exeter EX4 4QD, U.K.

and

YVES ROGER

Lab. Chimie Coordination Organique, Université de Rennes 1, Campus de Beaulieu, 35042 Rennes Cedex, France

Abstract—The octahedral tris-chelate complexes [M(tta)$_3$] (M = Al^{III}, Ga^{III}; tta = 2-thenoyltrifluoroacetone or 4,4,4-trifluoro-1-(2-thienyl)-1,3-butanedione) were isolated as mixtures of *cis*- and *trans*-isomers. Their fluxionality in solution was measured by ^{19}F NMR two-dimensional exchange spectroscopy and one-dimensional bandshape analysis. Rates of exchange between all four fluorine signals for a given temperature imply a common transition state for both the *cis–trans* isomerization and the Δ–Λ racemization processes. A bond rupture mechanism involving a trigonal bipyramidal or, more probably, a square planar transition state structure with a pendant axial ligand is proposed for the fluxion. The indium(III) complex [In(tta)$_3$] was also prepared but its fluxionality was too rapid to be followed by ^{19}F NMR spectroscopy. Activation energies [$\Delta G^{\ddagger}$ (298.15 K)] for the fluxions were 89.8±0.3 (Al^{III}) and 75.4±0.2 kJ mol^{-1} (Ga^{III}). ^{1}H and ^{19}F NMR data for the octahedral complex [Co(tta)$_3$], and the tetrahedral complexes [Be(tta)$_2$] and [Zn(tta)$_2$] are also reported.

The study of the fluxional behaviour of metal chelate complexes in the 1960s established NMR spectroscopy as an exceedingly powerful technique for probing stereochemical non-rigidity in molecules. Many classic dynamic NMR (DMNR) studies were made during the period 1960–1975 and those involving metal tris-chelate complexes have been reviewed in detail by Holm[1] and by Serpone and Bickley.[2] These early studies to identify the fluxional mechanism(s) operating in such complexes usually depended on accurate total bandshape analyses of complex ^{1}H NMR spectra. However, Fay and Piper[3,4] demonstrated the advantages of using ^{19}F NMR over ^{1}H NMR spectroscopy when the chelate ligands contained fluorine atoms, as in the case of the metal complexes of 1,1,1-trifluoro-2,4-pentanedione (tfac-H), namely [M(tfac)$_3$] (M = Al^{III}, Ga^{III} and In^{III}). However, these authors did not attempt any accurate treatment of the ^{19}F NMR bandshape changes with temperature and so were unable to deduce whether the rates of *cis–trans* isomerization and Δ–Λ racemization of these complexes were equal or not. A later study[5] on [Al(tfac)$_3$] and [Ga(tfac)$_3$] utilizing

* Dedicated to Eddie Abel, a greatly valued friend, collaborator and colleague.

† Author to whom correspondence should be addressed.

^{1}H total bandshape analysis of the ligand methyl signals was no more accurate as the bandshape changes were subtle and difficult to fit, even on the basis of a single magnitude of exchange rate constant for any given temperature (i.e. on the assumption of equal rates of isomerization and racemization). Without a precise knowledge of both rate processes little can be deduced about the mechanism of the fluxional rearrangement.

We have now employed the modern DNMR technique of two-dimensional exchange spectroscopy (2D-EXSY)[6–8] to measure rates of isomerization and racemization independently over a range of temperatures and can now offer more definitive conclusions on the activation energies and mechanism of the non-rigidity in some unsymmetrical tris-chelate complexes. The complexes chosen for study are those of 2-thenoyltrifluoroacetone (tta-H) and DNMR data are reported on the octahedral complexes $[M(tta)_3]$ (M = Co, Al, Ga and In), where *cis* and *trans* forms are possible (**1**).

We also report some ^{1}H and ^{19}F data on the tetrahedral complexes $[M(tta)_2]$ (**2**), where no isomerization is possible.

A wide range of metal complexes of tta are known, literature references to their previous preparations being given in the Experimental section (see later). Crystal structures of the tris octahedral complexes $[M(tta)_3]$ (M = Fe^{III},[9] In^{III}[9] and Ru^{III}[10]) have been reported but no studies made of their fluxionalities. In this present work, ^{1}H and ^{19}F NMR data are also reported for the four-coordinate tetrahedral complexes $[Be(tta)_2]$ and $[Zn(tta)_2]$ (**2**), which cannot undergo any detectable fluxionality. The crystal structures of the analogous *trans* planar complexes $[Pd(tta)_2]$[11] and $[Cu(tta)_2]$[12] have been described. In all the above-mentioned complexes, the tta ligand functions as a bidentate chelate ligand. However, there has also been a report of a complex which contains a bidentate tta and monodentate tta in the same structure, namely [Cu(2,2′-bipyridyl)$(tta)_2$].[13] This is a square pyramidal, five-coordinate complex in which the monodentate tta occupies the axial position.

EXPERIMENTAL

Materials

2-Thienyl-4,4,4-trifluoro-butane-2,2-dione (2-thenoyltrifluoroacetone) (tta-H) was used as supplied (Aldrich; m.p. 43.3–43.8°C, lit.[14] 42.5–43.2°C). The complexes were made by reported procedures and characterized by melting points (Table 1) and IR spectra. $[Co(tta)_3]$ was prepared from $Na_3[Co(CO_3)_3]\cdot 3H_2O$ by a method similar to that used by Bauer and Drinkard[15] for $[Co(acac)_3]$, and by Gordon and Holm[16] to make $[Co(Me_2CHCOCHCOMe)_3]$. The tta complexes of Be^{II},[17,18] Zn^{II},[19] Al^{III} [20–22] and In^{III} [9,23,24] were made by the general method[22] of treating a metal salt with the β-diketone in aqueous alcohol and buffering the solution with sodium acetate. $[Ga(tta)_3]$ was made by a variation on the reported procedure[25] in which an aqueous solution of the potassium salt of tta-H was added to a solution of gallium trichloride in ethanol. The complex precipitated from the aqueous alcoholic solution.

Spectra

All IR spectra of the complexes were recorded as KBr discs on a Nicolet Magna 550 FT-IR spectrometer in the range 4000–400 cm^{-1}.

All NMR spectra were recorded on a Bruker ACF-300 operating at 300 and 282 MHz for ^{1}H and ^{19}F nuclei, respectively. Spectra of the complexes were recorded as solutions in $CDCl_3$, $CDCl_2\cdot CDCl_2$ or CD_2Cl_2 (see Table 2). ^{1}H NMR shifts are expressed relative to Me_4Si ($\delta = 0$) and ^{19}F shifts relative to C_6F_6 ($\delta = 0$). The ^{27}Al spectrum recorded for $[Al(tta)_3]$ was measured at 78.2 MHz. The ^{27}Al shift was calculated relative to $[Al(H_2O)_6]^{3+}$ (see Table 2). ^{19}F 2D-EXSY spectra were obtained with the Bruker automation program NOESYPH with the pulse sequence *D*1-90°-*D*0-90°-*D*9-90°-FID. The relaxation delay *D*1 was 2.0 s and the evolution time had an initial value of 3×10^{-6}s. The mixing time *D*9 (t_m) was varied as shown in Table 3 between 0.1 and 3 s depending on the complex and temperature. The sizes of both frequency domains *F*1 and *F*2 were 512 words. The spectral width was 124 Hz and the number of pulse sequences per experiment was 16. Data processing incorporated a Gaussian window function in both frequency dimensions. Signal intensities in the two-dimensional contour plots were measured by row integration, averaging values of the four most appropriate rows. Rate data were computed using the authors' D2DNMR program.[26] NMR probe temperatures were varied using the standard B-VT 1000 accessory. Quoted temperatures are accurate to *ca* ± 1°C. NMR bandshape analyses were carried out with the authors' version of the standard DNMR3 program of Kleier and Binsch.[27]

RESULTS

All the tris-chelate octahedral complexes (**1**) were characterized by melting points (Table 1), IR spec-

Table 1. Synthesis and melting point data for $[M(tta)_3]$ complexes

Complex[a]	Yield (%)	Recrystallized from	M.p. (°C)	M.p. (°C)[b]
$[Co(tta)_3]$	94	toluene	204	188–189[20]
$[Be(tta)_2]$	29	ethanol	169.5–171.5	164;[17] 169–170[22]
$[Zn(tta)_2]$	91	ethanol	184–190	
$[Al(tta)_3]$	33	toluene–light petroleum	205	203–205;[22] 203–204[20]
$[Ga(tta)_3]$	76	toluene–light petroleum	183–185	
$[In(tta)_3]$	49	toluene–light petroleum	164–165	159;[23] 164.6±0.8[9]

[a] See Experimental section for preparative route.
[b] Superscripts give literature references.

Table 2. Static ^1H and ^{19}F NMR chemical shift data[a] for $[M(tta)_n]$ complexes

Complex	Solvent	^1H shifts, δ[b]				^{19}F shifts, δ[c]
		H(3)	H(4)	H(5)	CH(CO)	CF_3
trans-$[Co(tta)_3]$	$CDCl_3$ (^1H)	7.841	7.132	7.665	6.574	88.55
	$(CDCl_2)_2$ (^{19}F)	7.816	7.103	7.643	6.548	88.51
		7.794	7.097	7.619	6.548	88.37
cis-$[Co(tta)_3]$	$(CDCl_2)_2$	—	—	—	—	88.71
$[Be(tta)_2]$	$CDCl_3$	7.95	7.20	7.78	6.58	—
$[Zn(tta)_2]$	$CDCl_3$	7.86	7.18	7.73	6.45	—
trans-$[Al(tta)_3]$[d]	$CDCl_3$ (^1H)[e]	7.874	7.169	7.725	6.479	86.11
	$(CDCl_2)_2$ (^{19}F)	7.856	7.141	7.704	6.476	86.09
		7.842	7.135	7.670	6.466	85.94
cis-$[Al(tta)_3]$	$(CDCl_2)_2$	7.858	7.163	7.691	6.479(?)	86.26
trans-$[Ga(tta)_3]$	$CDCl_3$ (^1H)	7.885	7.180	7.751	6.447	86.78
	$CDCl_3$(^{19}F)	7.864	7.150	7.720	6.442	86.76
		7.855	7.147	7.700	6.431	86.66
cis-$[Ga(tta)_3]$	$CDCl_3$	7.870	7.176	7.729	6.45	86.85
cis/trans-$[In(tta)_3]$[f]	$CDCl_3$ (^1H)	7.85	7.15	7.71	6.40	87.19[g]
	CD_2Cl_2 (^{19}F)					

[a] Data recorded at 300 K except where otherwise stated.
[b] Relative to Me_4Si ($\delta = 0$). All thenoyl hydrogen signals are doublets of doublets with $^3J_{45} \sim 5$ Hz, $^3J_{34} \sim 4$ Hz and $^4J_{35} \sim 1$ Hz. All olefinic hydrogen signals are singlets.
[c] Relative to C_6F_6 ($\delta = 0$). All signals are singlets.
[d] ^{27}Al spectrum also recorded. One signal (half-height width ~200 Hz) detected at $\delta = -3.8 \pm 0.2$ relative to $[Al(H_2O)_6]^{3+}$ (assuming Ξ ref. = 26.057 MHz).
[e] ^1H data measured at 0°C.
[f] Data refer to exchange-averaged *cis–trans* species.
[g] At −100°C. Signal half-height width ~7 Hz.

tra and $^1H/^{19}F$ NMR spectra (Table 2). The bis-chelate tetrahedral complexes (**2**) of Be^{II} and Zn^{II} were characterized by ^1H NMR spectroscopy. Whereas these four-coordinate complexes do not display any structural isomerism, the unsymmetrical tris-chelate complexes can exist as both *cis*- and *trans*-isomers. NMR allows immediate distinction between these forms by virtue of their different symmetries. In the *cis*-isomer all three ligand environments are equivalent and therefore corresponding nuclei in different ligands are isochronous, whereas in the *trans*-isomer all three ligands are non-equivalent and sets of three ^1H or ^{19}F chemical shifts ensue.

The ^1H spectra of the complexes $[M(tta)_3]$ ($M = Co^{III}$, Al^{III}, Ga^{III} or In^{III}) possessed distinctive features depending on the transition metal. In the case of Co^{III}, the *trans*-isomer was predominant in

Table 3. Rate constants (s^{-1})[a] for isomerization/racemization of $[M(tta)_3]$ complexes derived from ^{19}F NMR 2D-EXSY experiments

Temp. (°C)	Mixing time t_m (s)	k_{21}	k_{31}	k_{41}	k_{23}[b]	k_{24}	k_{34}	$\langle k \rangle$[c]
$[Al(tta)_3]$[d]								
55	1.0	0.036	0.035	0.038	0.109	0.031	0.029	0.035
	2.0	0.037	0.037	0.039	0.088	0.033	0.031	
	3.0	0.040	0.038	0.037	0.072	0.032	0.029	
60	0.5	0.047	0.051	0.047	0.230	0.049	0.052	0.052
	1.0	0.052	0.053	0.056	0.138	0.053	0.047	
	2.0	0.054	0.052	0.053	0.113	0.057	0.052	
70	0.5	0.145	0.148	0.151	0.534	0.149	0.139	0.146
	1.0	0.144	0.152	0.152	0.366	0.145	0.135	
	2.0	0.152	0.158	0.142	0.280	0.144	0.141	
75	0.2	0.215	0.274	0.247	1.115	0.239	0.180	0.233
	0.4	0.221	0.261	0.242	0.841	0.240	0.203	
	0.8	0.243	0.255	0.232	0.563	0.235	0.226	
80	0.1	0.340	0.399	0.295	2.692	0.492	0.306	0.359
	0.2	0.321	0.376	0.335	1.766	0.435	0.333	
	0.4	0.336	0.345	0.327	1.098	0.394	0.348	
$[Ga(tta)_3]$[e]								
0	2.0	0.021	0.022	0.026	0.039	0.024	0.022	0.03
10	2.0	0.093	0.096	0.093	0.093	0.086	0.091	0.09
	1.0	0.086	0.081	0.086	0.098	0.077	0.084	
	0.5	0.057	0.064	0.079	0.086	0.062	0.078	
19	0.8	0.145	0.183	0.181	0.196	0.160	0.174	0.18
	0.4	0.134	0.166	0.178	0.275	0.182	0.153	
30	0.1	0.69	0.65	0.67	1.16	0.59	0.70	0.69
	0.2	0.64	0.67	0.60	0.96	0.60	0.65	
	0.4	0.60	0.63	0.64	0.77	0.63	0.62	

[a] See Fig. 4 for definitions of rate constants.

[b] Inaccurate value due to integration error of the two close signals 2 and 3 and not included in the averaging procedure.

[c] Averaged rate constant.

[d] Isomer populations, *cis* 16%, *trans* 84%, approximately temperature independent.

[e] Isomer populations, *cis* 13%, *trans* 87%.

solution as revealed by the three sets of chemical shifts associated with the thienyl ring hydrogens and the methine hydrogen. The thienyl signals appeared as doublets of doublets due to spin–spin coupling with other ring hydrogens, whereas the methine hydrogens were singlets. No evidence of any *cis*-isomer was found in the ^1H spectrum of $[Co(tta)_3]$, but its ^{19}F spectrum (see later) did indicate a very low population of *cis*-species. *Cis*-isomers were present to greater extents (*ca* 13–16%) in the solution ^1H spectra of the Al^{III} and Ga^{III} complexes. The high resolution spectrum of $[Ga(tta)_3]$ in $CDCl_3$ at 0°C is shown in Fig. 1. It consists of four overlapping AMX spin systems for the thienyl hydrogens. The dominant signals are again due to the *trans*-isomer but the less intense signals due to the *cis*-isomer can also be identified unambiguously. The assignments of the signals due to the H(3) and H(5) thienyl hydrogens in structures **1** and **2** were not obvious immediately. The assignments given in Fig. 1 and Table 2 are based on a nuclear Overhauser enhancement (NOE) difference experiment[28] on a solution of the $[Be(tta)_2]$ complex, where a strong enhancement due to cross-relaxation was detected between the methine hydrogen and the highest frequency thienyl ring signal, which was therefore assigned to the H(3) hydrogen. This assignment, which was in agreement with an earlier one based on an INDOR experiment,[17] was assumed valid for all the tta complexes studied, as the ligand geometry is unlikely to change drastically for different metal coordinations.

The observation of separate ^1H signals for *cis*- and *trans*-isomers indicated that any isomerization was slow on the ^1H NMR chemical shift time scale at ambient temperatures. Some slight dynamic broadening was detected in the spectrum of $[Ga(tta)_3]$ at room temperature and cooling to 0°C was required to produce a true "static" spectrum

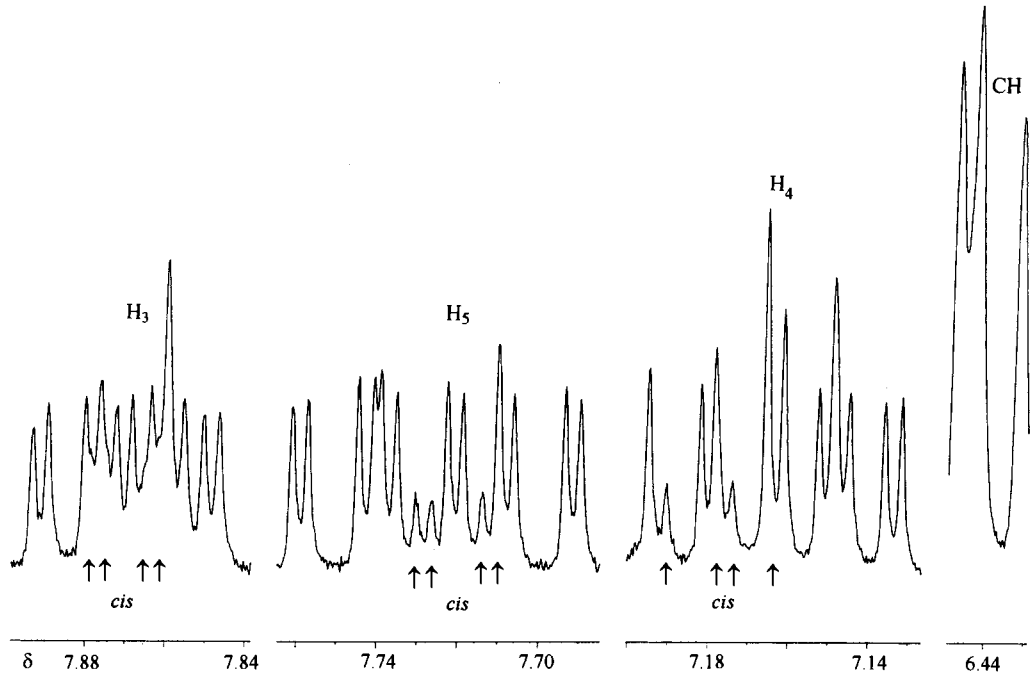

Fig. 1. 300 MHz ^{1}H NMR spectrum of [Ga(tta)$_3$] in $CDCl_3$ at 0°C. Signals due to minor *cis*-species indicated by arrows.

(Fig. 1). The case of [In(tta)$_3$], however, was quite different, with a single set of signals for thienyl and methine hydrogens indicating rapid *cis–trans* isomerization (Fig. 2a).

All these findings were substantiated by the ^{19}F spectra of these complexes. For the Al^{III} and Ga^{III} complexes, three equal intensity signals were detected for the *trans*-species and a considerably weaker signal, to higher frequency of the other three, was ascribed to the *cis*-isomer. The spectrum of the Al^{III} complex is shown in Fig. 3. In the case of the Co^{III} complex, the *cis* signal constituted only *ca* 1% of the total spectral line intensity. In the spectrum of the In^{III} complex (Fig. 2b) a single ^{19}F signal confirms the assumption of rapid *cis–trans* isomerization. The major advantage of using ^{19}F NMR over ^{1}H NMR in distinguishing between *cis*- and *trans*-isomers and following their interconversions was made originally by Fay and Piper[3,4] on [M(tfac)$_3$] complexes, and is confirmed here for the analogous [M(tta)$_3$] complexes. Whereas ^{1}H chemical shift distinctions between corresponding signals of *cis*- and *trans*-isomers are only of the order of 0.01–0.03 ppm, in their ^{19}F spectra such distinctions are approximately 10-fold greater, i.e. ^{19}F signal spreads are 0.1–0.15 ppm (Table 2). A further advantage is that all ^{19}F signals of the ligand CF_3 groups are non-overlapping singlets and this allows the application of the 2D-EXSY technique for measuring rates of exchange between the set of ^{19}F signals.

Isomerization/racemization of [M(tta)$_3$] *complexes*

The temperature variation of the ^{19}F spectra of the [M(tta)$_3$] complexes depended greatly on the nature of the transition metal. In the case of [Co(tta)$_3$], warming a $(CDCl_2)_2$ solution of this complex to *ca* 140°C led to an increased percentage of the *cis*-isomer to *ca* 17%. Some signal broadening was also detected but this was attributed to dissociation rather than isomerization/racemization, since on cooling the sample back to room temperature a free ligand CF_3 signal appeared at δ 86.17. These observations confirm the expected stereochemical rigidity of Co^{III} complexes.[1] Any isomerization/racemization which occurs is too slow to be measured by variable temperature NMR on an equilibrium isomeric mixture. A time-dependent NMR study of the rate of change of either pure *cis*- or *trans*-isomers would be required, analogous to that performed by Fay and Piper.[4]

^{19}F NMR spectra of solutions of [Al(tta)$_3$] and [Ga(tta)$_3$] displayed exchange broadening on warming, leading to eventual coalescence and sharpening of all four ^{19}F signals. These changes were associated with combined iso-

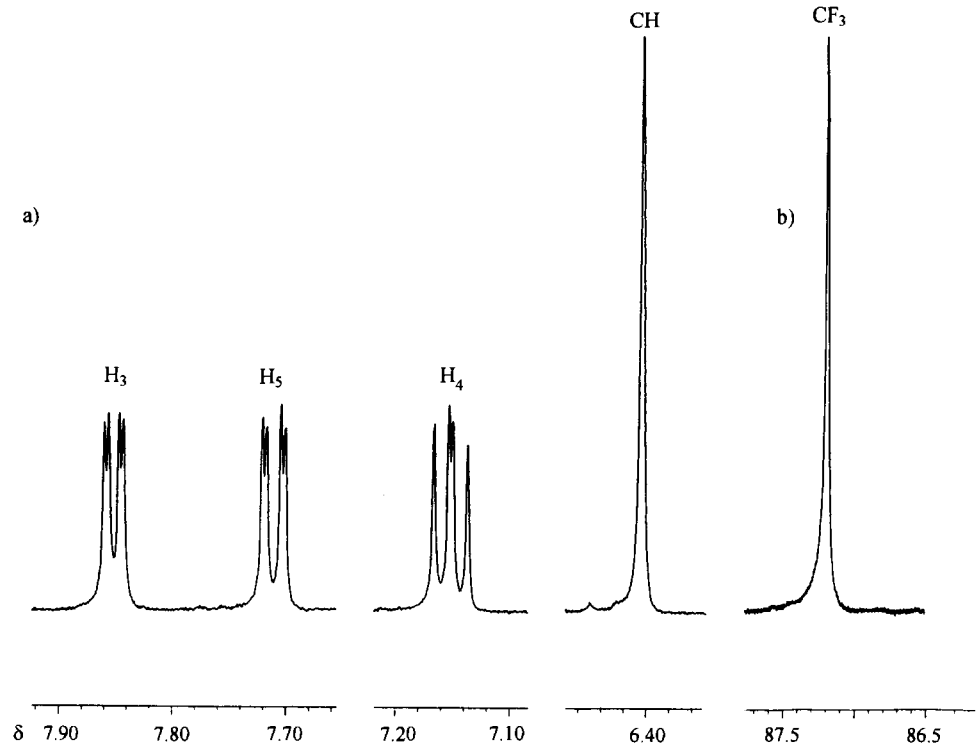

Fig. 2. (a) 300 MHz ^{1}H NMR spectrum of [In(tta)$_3$] in $CDCl_3$ at 300 K. (b) 282 MHz ^{19}F NMR spectrum in CD_2Cl_2 at 173 K.

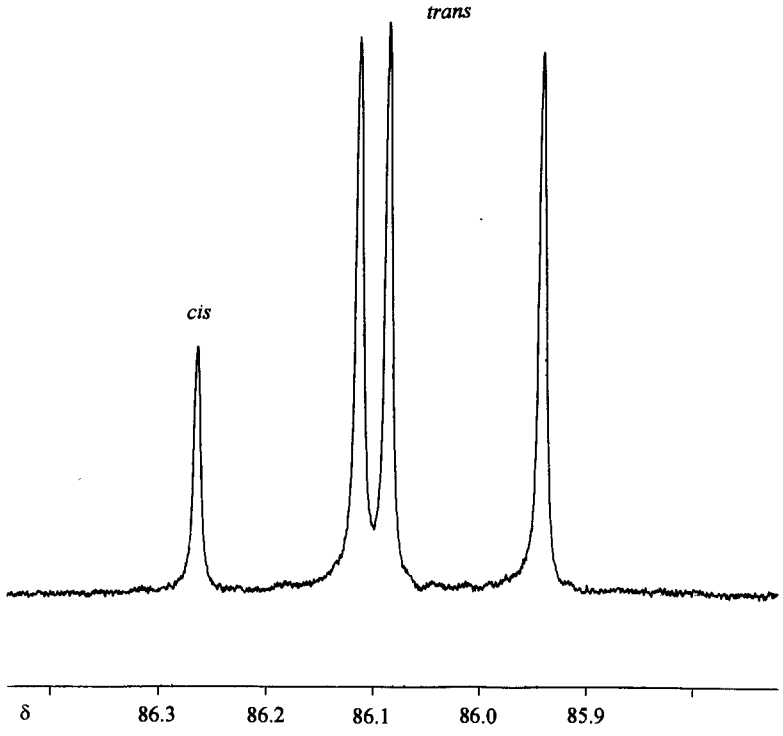

Fig. 3. 282 MHz ^{19}F NMR spectrum of [Al(tta)$_3$] in $(CDCl_2)_2$ at 300 K.

merization/racemization, and rates were measured accurately as described below.

The ^{19}F spectrum of [In(tta)$_3$] in CD_2Cl_2 solution consisted of a single signal down to a temperature

of −100°C (Fig. 2b), indicating rapid fluxional rearrangements which did not lend themselves to quantitative measurement.

[Al(tta)$_3$]

The ambient temperature ^{19}F spectrum of this complex consists of four signals, numbered 1–4, as shown schematically in Fig. 4. Signal 1 is associated with the *cis*-isomer and signals 2–4 with the *trans*-isomer. Exchange between these four signals is defined in terms of six forward and six reverse rate constants. Isomerization rates are given by k_{12}, k_{13} and k_{14} (*cis* → *trans*), and by k_{21}, k_{31} and k_{41} (*trans* → *cis*), these two sets being related by the chemical equilibrium relationships $p_1k_{12} = p_2k_{21}$, etc. where p_1 and p_2 are the populations of sites 1 and 2, respectively. Racemization rates are given by k_{23}, k_{24} and k_{34} or by k_{32}, k_{42} and k_{43}, these sets being equivalent as the populations of sites 2, 3 and 4 are equal. Rates of isomerization and racemization may be equal or unequal at any given temperature. Previous studies on related unsymmetrical tris-chelate complexes have been either approximate or have relied on total ^{1}H NMR bandshape analysis to decide between combinations of rate constants. This has often proved to be very difficult because of the very subtle differences in line shapes predicted for different cases. Previous studies of Fay and Piper[3,4] and others[5,21] have suggested a common transition state for both processes, but this has not been proved. To test this hypothesis it is necessary to show that, at a given temperature, the rate of racemization of the *trans*-isomer (as measured by the rate of exchange between its three ^{19}F signals) is equal to the rate of conversion to the *cis*-isomer. In other words, the rate constants k_{23}, k_{24}, k_{34}, k_{21}, k_{31} and k_{41} need to be measured individually and shown to be equal within experimental uncertainties.

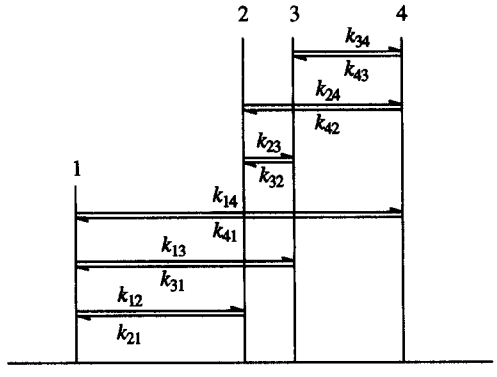

Fig. 4. Schematic representation of the isomerization and racemization rate constants associated with the ^{19}F NMR signals of *cis*- and *trans*-[M(tta)$_3$] complexes.

This may be accomplished by 2D-EXSY ^{19}F NMR experiments where exchange rates can be deduced from the relative intensities of diagonal signals and cross peaks in the two-dimensional NMR contour plot.[6–8] Such experiments were performed on [Al(tta)$_3$] in $(CDCl_2)_2$ solution at five different temperatures between 55 and 80°C. The spectrum at 80°C is shown in Fig. 5. For each temperature the mixing time chosen for the EXSY pulse sequence was varied in order to test the reproducibility of the data. The results are given in Table 3. It can be seen that all rate constants, with the exception of k_{23}, are of very similar magnitude. Values of k_{23} are invariably higher and this anomaly can be traced back to the two-dimensional NMR contour plots when the closeness of signals 2 and 3 cause their cross peaks to overlap slightly with the diagonal signals and so reduce the accuracy of integrations of these signals. It was therefore felt entirely justifiable to omit values of k_{23} when averaging the rate data for any temperature. Averaged values, $\langle k \rangle$, are given in Table 3. The values obtained for the five different temperatures were then incorporated in an Eyring plot ($\ln k/T$ against $1/T$). A good straight line was achieved, which enabled values of k to be extrapolated into the higher temperature range (Table 4). One-dimensional ^{19}F spectra of [Al(tta)$_3$] were then recorded in the temperature range ambient to 145°C and total lineshapes fitted, with the DNMR3 program, using the k values extrapolated from the 2D-EXSY experiments. Excellent fittings of experimental and computer-simulated spectra were achieved at all temperatures (Fig. 6), confirming that at any temperature a single magnitude of rate constant can define fully the fluxionality occurring.

[Ga(tta)$_3$]

The same procedure for extracting rate data from ^{19}F 2D-EXSY spectra was adopted for the Ga^{III} complex, the main difference from the Al^{III} study being the temperature range over which measurements were taken. The isomerization/racemization process is more facile for Ga^{III} than for Al^{III} and so 2D-EXSY spectra were taken in the below-ambient temperature range 0–30°C (Table 3), and one-dimensional bandshape analysis performed in the range 40–110°C (Table 4). Again, k values based on extrapolations of values measured by 2D-EXSY experiments produced very good fittings of experimental and theoretical lineshapes. In this case it should be noted that all six rate constants obtained from the 2D-EXSY spectra were included in the

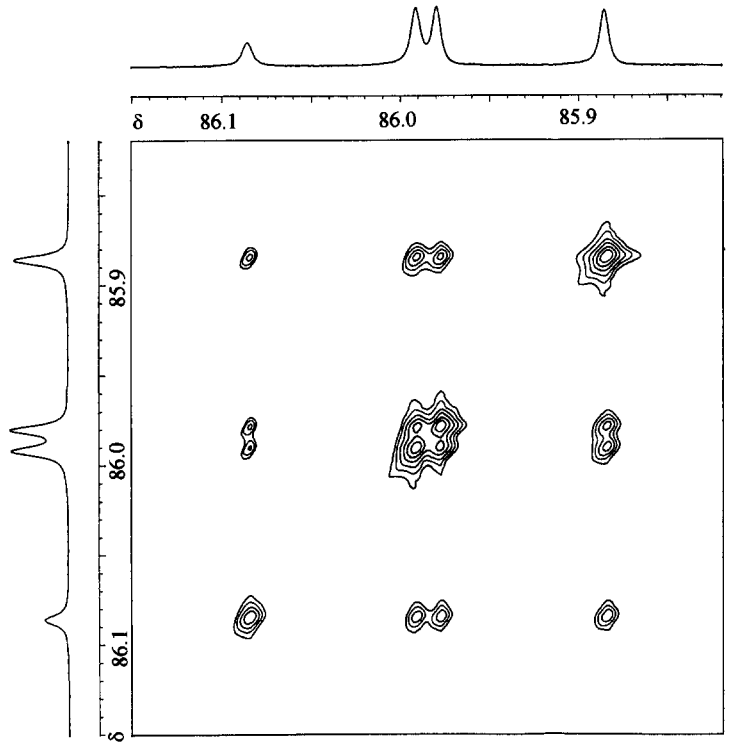

Fig. 5. 300 MHz ^{1}H 2D-EXSY NMR spectrum of [Al(tta)$_3$] in $(CDCl_2)_2$ at 80°C. Mixing time t_m = 0.4 s.

Table 4. Rate constants[a] used in the bandshape analyses of the ^{19}F NMR spectra of [M(tta)$_3$] complexes

[Al(tta)$_3$][b,c]		[Ga(tta)$_3$][d]	
Temp. (°C)	k (s^{-1})	Temp. (°C)	k (s^{-1})
90	0.84	40	1.63
100	1.9	50	3.97
110	4.1	55	6.1
115	6.0	60	9.2
120	8.6	65	13.8
125	12.3	70	20.2
130	17.3	75	29.7
135	24.1	80	42.8
140	33.6	90	86.9
145	46.3	100	169.3
		110	319.6

[a] Extrapolated values of 2D-EXSY-derived rate constants (Table 2). Accuracy ± 10%.

[b] Fittings of experimental and computer-simulated spectra shown in Fig. 6.

[c] Isomer populations, *cis* 15.3%, *trans* 84.7% (90°C) changing to *cis* 16.8%, *trans* 83.2% (145°C).

[d] Isomer populations, *cis* 13.6%, *trans* 86.4% (40°C) changing to *cis* 16.6%, *trans* 83.4% (110°C).

averaging procedure, as the k_{23} values appeared less spurious than in the case of [Al(tta)$_3$].

DISCUSSION

The variation of exchange rate constants with temperature enabled activation energy data for the isomerization/racemization process for [Al(tta)$_3$] and [Ga(tta)$_3$] to be calculated (Table 5). The $\Delta G^{\ddagger}$ value for [Al(tta)$_3$] was somewhat higher than the previous approximate value based on the coalescence temperature at 115°C.[21] The fluxional rates of the Co^{III} and In^{III} complexes were outside the range of NMR detection, being too slow and too fast, respectively. Activation energies, expressed either as E_a, $\Delta H^{\ddagger}$ or $\Delta G^{\ddagger}$ values, followed the same trend as found for the tfac complexes, namely Co^{III} $\gg$ Al^{III} > Ga^{III} $\gg$ In^{III}. This may be rationalized in terms of increasing radii of the metal ion within Group III and, for Co^{III}, the expected inertness of its d^6 low spin electronic configuration.

A comparison with the data of Grossmann and Haworth[5] showed significantly lower values than for the corresponding tfac complexes. The Fay and Piper data on these complexes were less accurate and no very meaningful comparisons can be made. The activation entropies, $\Delta S^{\ddagger}$, of the present data are small and negative (Table 5), in contrast to those of Grossmann and Haworth,[5] who argued that their small positive values support a bond-rupture mechanism for the fluxionality. However, accurate values of $\Delta S^{\ddagger}$ are exceedingly difficult to

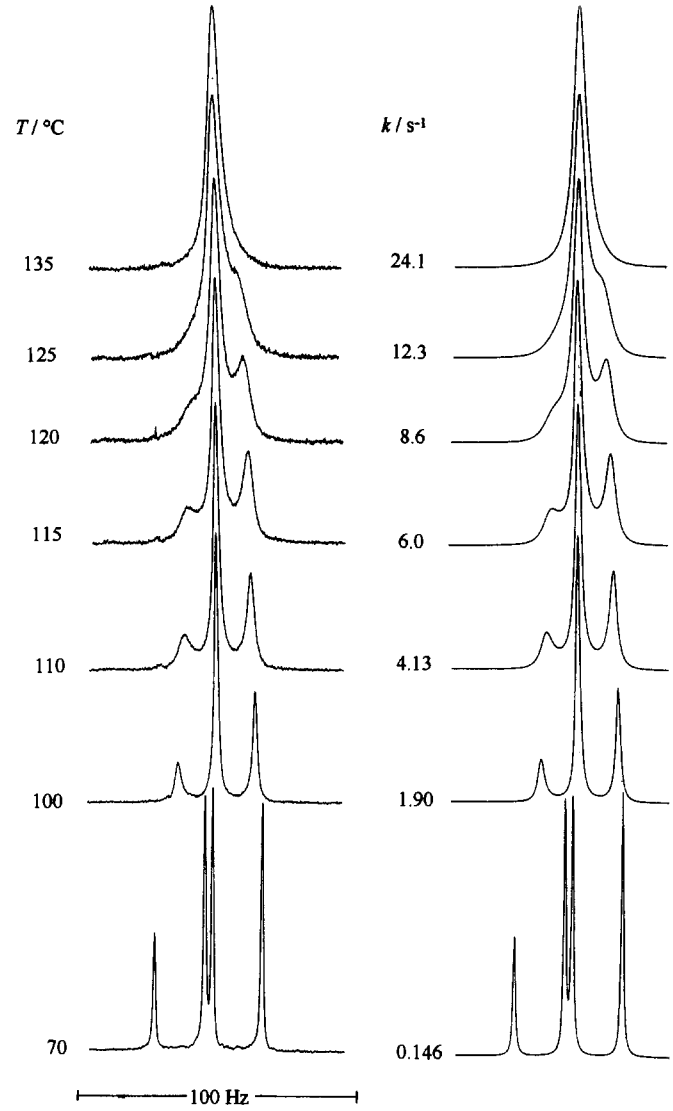

Fig. 6. Experimental and computer-stimulated ^{19}F spectra of $[Al(tta)_3]$. "Best-fit" rate constants shown are those based on extrapolations of the lower temperature 2D-EXSY values.

measure by NMR bandshape analysis[29] and, in our view, the only information that can be derived from small magnitudes of $\Delta S^{\ddagger}$ (positive or negative) is that a dissociation mechanism is not supported.

The most important finding of this present work is that isomerization and racemization of $[M(tta)_3]$ ($M = Al^{III}$ or Ga^{III}) complexes occur in a single concerted step involving a single type of transition state. Much attention has been given previously to possible mechanisms of fluxionality in tris-chelate complexes.[1-4] Two categories of intramolecular mechanism have been proposed, namely those involving momentary rupture of a metal–ligand bond and those that involve ligand twisting without any bond rupture. The bond rupture mechanism (Fig. 7) may involve either a trigonal bipyramidal (tbp) intermediate with a pendant equatorial or axial ligand, or a square pyramidal (sp) intermediate with a pendant axial ligand. It has been shown previously[1,2,4] that the mechanism involving a tbp intermediate with a pendant equatorial ligand (Fig. 7a) does not lead to any racemization ($\Delta \rightleftharpoons \Lambda$) and so this can be excluded in the present context. The possible twist mechanisms are of two types, namely a twist to a rhombic transition state of near C_{2v} symmetry and a twist to a trigonal transition state of near D_{3h} symmetry (Fig. 8). It has been shown that the trigonal twist mechanism (Fig. 8b) leads to racemization only and so this can also be excluded in the cases of $[M(tfac)_3]$ and $[M(tta)_3]$ complexes.

Fay and Piper suggested that a distinction between bond rupture and twist mechanisms could be made on the basis of solvent dependence of the

Table 5. Activation energy data for the isomerization/racemization of $[M(L—L')_3]$ complexes

Complex	Solvent	E_a (kJ mol^{-1})	$\log_{10}(A)$ (s^{-1})	$\Delta H^{\ddagger}$ (kJ mol^{-1})	$\Delta S^{\ddagger}$ (J K^{-1} mol^{-1})	$\Delta G^{\ddagger a}$ (kJ mol^{-1})	Ref.
$[Al(tta)_3]$	$(CDCl_2)_2$	91.5±2.1	13.1±0.3	88.7±2.1	−3.7±6.2	89.8±0.3	This work
$[Al(tta)_3]$	$(CDCl_2)_2$					84.9[b]	21
$[Ga(tta)_3]$	$CDCl_3$	74.7±4.3	12.7±0.8	72.3±4.2	−10.3±1.48	75.4±0.2	This work
$[In(tta)_3]$	CD_2Cl_2	$<\sim 40$				$<\sim 40$	This work
$[Al(tfac)_3]$	[c]	118±11	17.0±1.5	114±11	68±29	93.7±0.4	5
$[Al(tfac)_3]$	$CDCl_3$	98±8				82±7[d]	4
$[Ga(tfac)_3]$	[c]	92.9±0.4	15.2±0.1	91.2±0.4	41.4±0.9	78.9±0.4	5
$[Ga(tfac)_3]$	$CDCl_3$	87±7				72±6[e]	4
$[In(tfac)_3]$	$CDCl_3$	<56±4				<46±4	4

[a] Calculated for 298.15 K unless otherwise stated.
[b] For a coalescence temperature of 115°C.
[c] Solvent not known.
[d] For a coalescence temperature of 103°C.
[e] For a coalescence temperature of 61.5°C.

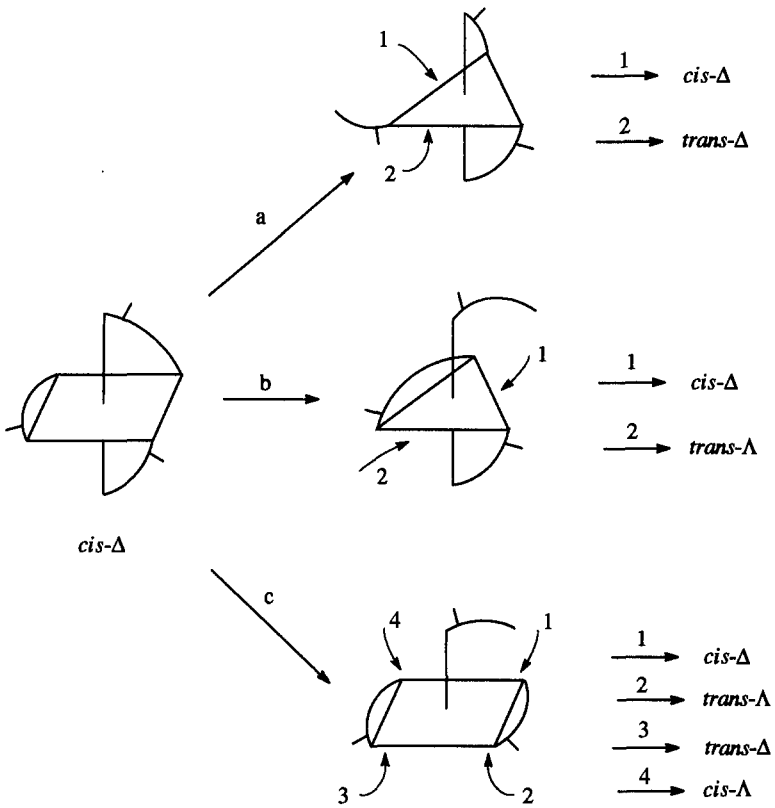

Fig. 7. Stereochemical rearrangement of a *cis*-Δ isomer of an $[M(L—L')_3]$ complex via a bond rupture mechanism involving a trigonal bipyramidal intermediate with pendant equatorial ligand (a), a trigonal bipyramidal intermediate with pendant axial ligand (b) and a square pyramidal intermediate with a pendant axial ligand (c). The numbers label possible sites for reattachment of the end of the ligand.

fluxional rate. They found for the $[M(tfac)_3]$ (M = Al^{III} or Ga^{III}) complexes that the free energy of activation at the coalescence temperature decreased with increasing dielectric constant of solvent, which they interpreted as supporting a bond-rupture mechanism through the greater charge sep-

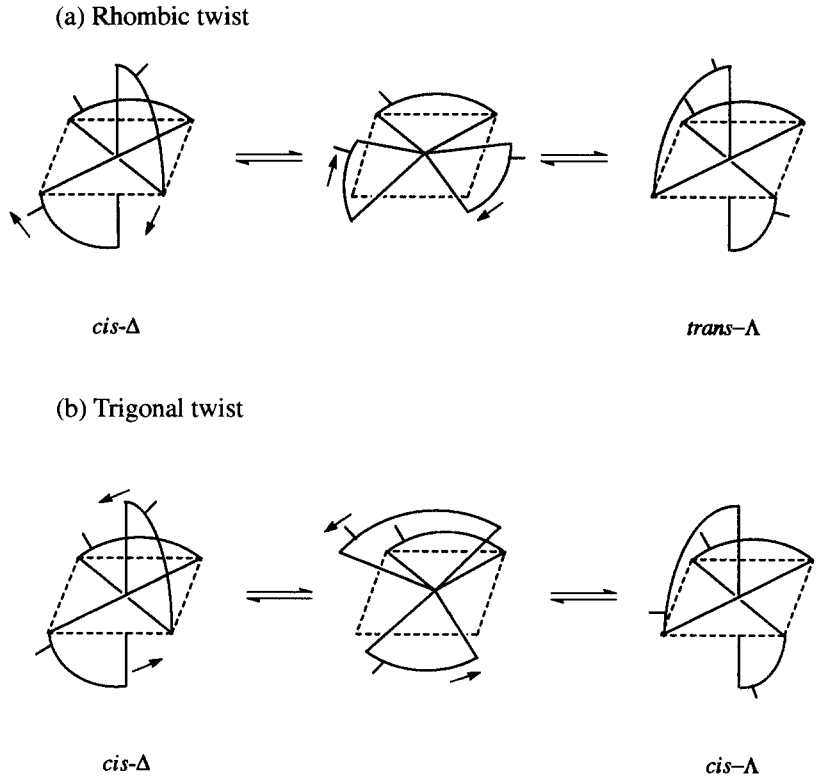

Fig. 8. Stereochemical rearrangement of a *cis*-Δ isomer of an $[M(L—L')_3]$ complex via a rhombic twist (a) and a trigonal twist (b).

aration and greater solvation of the transition state. In contrast, the rhombic twist mechanism predicts smaller charge separation in its transition state.

This idea was tested in the present complexes by examining the effect of solvent on the ^{19}F spectrum of $[Ga(tta)_3]$. On changing from $(CDCl_2)_2$ to DMSO-d_6 there were gross changes in the spectrum, namely, in ^{19}F chemical shifts, isomer populations (the *cis*-isomer now being present to the extent of 21%) and, particularly, the exchange rates of the four ^{19}F signals. An appropriate calculation showed that at *ca* 55°C the rate of isomerization/racemization increased about 10-fold (from ~6 to 67 s^{-1}) on changing solvent from $(CDCl_2)_2$ (dielectric constant 8.2) to DMSO-d_6 (dielectric constant 46.7). This evidence therefore supports the bond-rupture mechanism for the tta complexes.

Further support for this type of mechanism arises from a detailed permutational analysis of the mechanisms of stereoisomerism on aluminium tris-substituted β-diketonate complexes by Springer *et al.*[30] Whereas Fay and Piper considered that bond rupture might occur via a tbp or sp intermediate, the analysis of Springer *et al.*[30] favours an sp intermediate (Fig. 7c) with bond rupture taking place at the CF_3 end of the β-diketone ligand. Our present results fully accord with such a mechanism occurring in $[M(tta)_3]$ complexes. However, it should be noted that crystal structure data of other $[M(tta)_3]$ complexes do not show the M—O bond of the CF_3 end of the β-diketone to be invariably longer, and therefore weaker, than the other bond. The precise location of the bond-rupture process is therefore not totally certain, though it is perhaps worth noting that in the $[Cu(2,2'\text{-bipyridyl})(tta)_2]$ complex[13] the monodentate tta is coordinated via the thenoyl oxygen, suggesting that this end of the tta is less prone to bond rupture.

Acknowledgement—The work carried out by one of us (Y. R.) was in conjunction with the ERASMUS exchange scheme.

REFERENCES

1. R. H. Holm, in *Dynamic Nuclear Magnetic Resonance Spectroscopy* (Edited by L. M. Jackman and F. A. Cotton), Ch. 9. Academic Press, New York (1975).
2. N. Serpone and D. G. Bickley, *Prog. Inorg. Chem.* 1972, **17**, 391.
3. R. C. Fay and T. S. Piper, *J. Am. Chem. Soc.* 1963, **85**, 500.

4. R. C. Fay and T. S. Piper, *Inorg. Chem.* 1964, **3**, 348.
5. D. L. Grossmann and D. T. Haworth, *Inorg. Chim. Acta* 1984, **84**, L17.
6. R. Willem, *Prog. NMR Spectrosc.* 1987, **20**, 1.
7. C. L. Perrin and T. J. Dwyer, *Chem. Rev.* 1990, **90**, 935.
8. K. G. Orrell, V. Šik and D. Stephenson, *Prog. NMR Spectrosc.* 1990, **22**, 141.
9. H. Soling, *Acta. Chem. Scand. Ser. A* 1976, **30**, 163.
10. S. Aynetchi, P. B. Hitchcock, E. A. Seddon, K. R. Seddon, Y. Z. Yousif, J. A. Zora and K. Stuckey, *Inorg. Chim. Acta* 1986, **113**, L 7.
11. C. E. Urdy, *Cryst. Struct. Commun.* 1976, **5**, 527.
12. J. A. Pretorius and J. C. A. Boeyens, *J. S. Afr. Chem. Inst.* 1977, **30**, 153.
13. Z. Xu, S.-H. Gou, X.-Z. You, S.-X. Liu, C.-C. Lin, Y.-P. Yu and D.-L. Zhu, *Acta Cryst.* (*Cryst. Struct. Commun.*) 1991, **C47**, 81.
14. J. C. Reid and M. Calvin, *J. Am. Chem. Soc.* 1950, **72**, 2948.
15. H. F. Bauer and W. C. Drinkard, *J. Am. Chem. Soc.* 1960, **82**, 5031.
16. J. G. Gordon II and R. H. Holm, *J. Am. Chem. Soc.* 1970, **92**, 5310.
17. A. Barabas, *Rev. Roum. Chim.* 1972, **17**, 1997.
18. D. T. Haworth and M. Das, *J. Fluorine Chem.* 1984, **26**, 331.
19. K. S. Patel, *J. Inorg. Nucl. Chem.* 1980, **42**, 1235.
20. K. S. Patel and A. A. Adimado, *J. Inorg. Nucl. Chem.* 1980, **42**, 1241.
21. M. Das, D. T. Haworth and J. W. Beery, *Inorg. Chim. Acta* 1981, **49**, 17.
22. E. W. Berg and I. T. Truemper, *J. Phys. Chem.* 1960, **64**, 487.
23. G. M. Tanner, D. G. Tuck and E. J. Wells, *Can. J. Chem.* 1972, **50**, 3950.
24. M. Das, *J. Inorg. Nucl. Chem.* 1981, **43**, 3412.
25. Z. Jablonski, I. Rychlowska-Himmel and M. Dyrek, *Spectrochim. Acta* 1979, **35A**, 1297.
26. E. W. Abel, T. P. J. Coston, K. G. Orrell, V. Šik and D. Stephenson, *J. Magn. Reson.* 1986, **70**, 34.
27. D. A. Kleier and G. Binsch, DNMR3, Program 165, Quantum Chemistry Program Exchange, Indiana University, U.S.A. (1970).
28. H. Friebolin, *Basic One- and Two-Dimensional NMR Spectroscopy*, 2nd, ed, Ch. 10. VCH, Weinheim (1993).
29. J. Sandström, *Dynamic NMR Spectroscopy*, Ch. 7. Academic Press, London (1982).
30. M. Pickering, B. Jurado and C. S. Springer Jr., *J. Am. Chem. Soc.* 1976, **98**, 4503.